

# Steady State Analysis of Self-Excited Induction Generator for Isolated System

A. M. Agwa

Department of Electrical Engineering, Al-Azhar University, Cairo, Egypt

**Abstract**—Self-excited induction generators (SEIG) are induction generators with capacitor excitation. Self-excited induction generators (SEIG) are extensively utilized in non-conventional energy systems such as wind, small hydro, biogas, etc. Steady state analysis for such machines is necessary to assess the performance under actual operating conditions. A 1.8 kW induction machine excited with symmetrical capacitor bank in isolated system, was the subject of investigation in this paper. A simple mathematical model is proposed to calculate the steady-state performance of self-excited induction generator by nodal admittance model. MATLAB programming is used to solve the proposed model. The results obtained by MATLAB programming are compared with experimental results. The results confirm the validity and accuracy of the MATLAB based modeling of self-excited induction generator.

**Keywords**—Steady State Analysis, Self Excited Induction Generator, Admittance Model.

## NOMENCLATURES

$f_s$  synchronous frequency  
 $f_b$  base frequency  
 $f_1$  generated frequency  
 $f$  per unit frequency  
 $n$  rotational speed  
 $v$  per unit rotational speed  
 $s$  slip  
 $p$  number of pole pairs  
 $R$  load resistance per phase  
 $X$  load reactance per phase  
 $Z$  load impedance per phase  
 $R_1$  stator resistance per phase  
 $R_{21}$  rotor resistance per phase, referred to stator  
 $X_1$  stator reactance per phase  
 $X_{21}$  rotor reactance per phase, referred to stator  
 $X_m$  maximum saturated magnetizing reactance per phase at rated frequency  
 $X_{m-s}$  saturated magnetizing reactance per phase at rated frequency  
 $R_{e+h}$  core loss resistance per phase  
 $C$  capacitance for self excitation per phase  
 $C_{min}$  minimum self excitation capacitance per phase  
 $X_C$  capacitive reactance due to  $C$  at rated frequency  
 $X_{C-max}$  maximum self excitation capacitive reactance corresponding to  $C_{min}$   
 $R_L$  resistance of equivalent impedance of capacitor and load  
 $X_L$  reactance of equivalent impedance of capacitor and load  
 $R_{1L}$  resistance of equivalent impedance of capacitor, load and stator  
 $X_{1L}$  resistance of equivalent impedance of capacitor, load and stator  
 $E_1$  air-gap voltage per phase at rated frequency  
 $E_a$  air-gap voltage per phase for frequency  $f$   
 $V_1$  terminal voltage per phase  
 $I_1$  stator current per phase  
 $I_2$  rotor current per phase, referred to stator

$I_m$  magnetizing current per phase  
 $I_{e+h}$  core loss current per phase  
 $I_L$  load current per phase  
 $I_C$  capacitor current  
 $P_{out}$  output power  
 $M_0, M_1$  and  $M_2$  constants dependent on the induction machine  
 $N_0, N_1$  and  $N_3$  constants dependent on the induction machine  
 $P_n$  rated power  
 $V_s$  supply voltage  
 $I_{a n}$  rated armature current  
 $V_{f n}$  rated field voltage  
 $I_{a n}$  rated field current

## I. INTRODUCTION

An externally driven induction machine with a suitable value of capacitor bank can be used as a generator. The generators that work based on this phenomenon, are known as self-excited induction generators (SEIG). The SEIG have been found convenient for energy generation for remote areas that cannot be accessed to electric public grid. The SEIG has many advantages over the synchronous generator: simple construction, ruggedness, absence of DC power supply for excitation, no synchronization problems, reduced price and maintenance cost, good over speed capability and self short-circuit protection capability and reduced size ruggedness. But the SEIG exhibit poor performance in terms of voltage and frequency under frequent variations of operating speeds, which is a common feature in wind energy conversion [1]. Voltage and frequency of SEIG, depend on the prime mover speed, capacitor bank and load [2]. Use of an induction machine as a generator is becoming more and more popular for the renewable sources [3].

## II. INDUCTION GENERATORS

Induction generators (IG) need magnetizing current for excitation and external prime-over without anything further. When these generators are connected in power systems, then reactive power for magnetization can be received by grid itself. But a stand-alone operation generator can be operated in self-excitation mode by connecting a capacitor in parallel with magnetizing reactance [4]. Main drawback of induction generators is reactive power consumption and no control on terminal voltage and frequency. Maintaining the Integrity of the Specifications

## III. STEADY STATE PERFORMANCE OF SELF EXCITED INDUCTION GENERATOR

Various analytical methods (models) have been developed in order to predict the steady state performance of SEIG [5]. Among them, two are predominant:

- The impedance model.
- The admittance model.

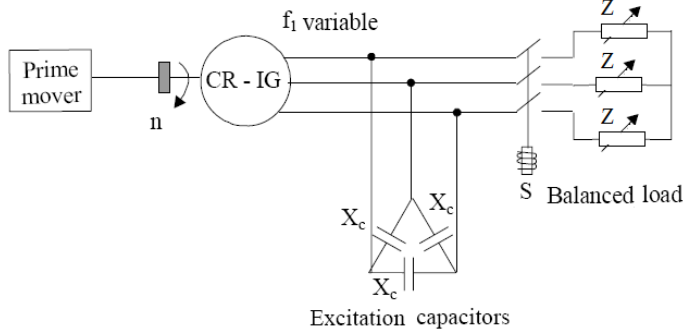


Fig. 1: General scheme of SEIG with balanced load

The impedance model is based on the single-phase equivalent circuit shown in Fig. 1, which, in general, is expressed in per unit terms:

$$f = \frac{\text{frequency}}{\text{rated frequency}}; f = \frac{f_1}{f_b} \quad (1)$$

$$v = \frac{\text{speed}}{\text{synchronous speed}}; v = \frac{n/60}{f_b/p} \quad (2)$$

The final form of the circuit is shown in Fig. 2. The load, the presence of core loss resistance  $R_{e+h}$  (which may also vary slightly with frequency  $f$ ), the nonlinearity of magnetizing reactance dependence on magnetizing current  $X_{m-s}(I_m)$  with the unknowns  $X_{m-s}$  (the real output is  $V_1$ ) and  $f$  makes the solving of this model possible only through a numerical procedure [6-8]. Once  $X_{m-s}$  and  $f$  are calculated the entire circuit model may be solved in a straightforward manner.

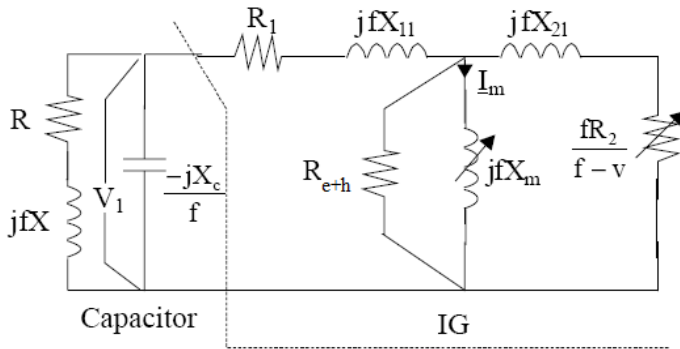


Fig. 2: The impedance model of SEIG

Fifth or fourth order polynomial equations in  $f$  or  $X_{m-s}$  are obtained from the conditions that the real and imaginary parts of the equivalent impedance are zero. Rather recently a fairly general solution of the impedance model, based on the optimization approach has been introduced [9].

However, the high order of system nonlinearity prevents an easy understanding of performance sensitivity to various parameters. In search of a simpler solution, the admittance model has been proposed [10].

While the  $X_{m-s}$  equation is simple, calculating  $f$  involves a complex procedure. In [11, 12] admittance models (that lead to quadratic equations for the unknowns) are obtained for balanced resistive load with neglecting the core loss resistance for simplicity.

In this paper admittance model is obtained for balanced load with taking the core loss resistance into consideration. The agreement of theoretical results obtained here with the experimental measurements, is better than that obtained using some other models.

#### IV. THE SECOND ORDER SLIP EQUATION MODEL FOR STEADY STATE

The second order equation model may be obtained from the standard circuit shown in Fig. 3.

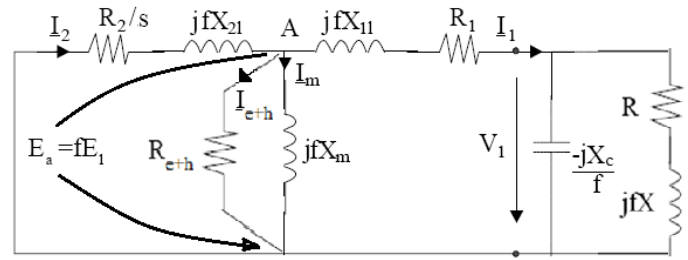


Fig. 3: Equivalent circuit of SEIG with slip  $s$  and frequency  $f$  (p.u.) shown

The slip is negative for generator mode:

$$s = \frac{f - v}{f} \quad (3)$$

The airgap voltage  $E_a$  for frequency  $f$  (in p.u.):

$$E_a = f E_1 = I_2 \left( \frac{R_2}{s} + jX_{21} \right) \quad (4)$$

where  $E_1$  = airgap voltage at rated frequency.

For accuracy, the core loss resistance is taken into account. From no-load test, the equivalent core loss resistance  $R_{e+h}$  as function of the airgap voltage  $E_1$ , is computed as following:

$$R_{e+h} = N_0 + N_1 E_1 + N_2 E_1^2 \quad (5)$$

where  $N_0, N_1$  and  $N_2$  are constants dependent on the design and material of the machine.

The parallel capacitor-load circuit may be transformed into a series one as following:

$$R_L - jX_L = \frac{(R + jfX)(-j\frac{X_C}{f})}{R + jfX - j\frac{X_C}{f}} \quad (6)$$

$$R_L = \frac{RX X_C - \frac{R X_C}{f} (fX - \frac{X_C}{f})}{R^2 + (fX - \frac{X_C}{f})^2} \quad (7)$$

$$X_L = \frac{X X_C \left( fX - \frac{X_C}{f} \right) + \frac{R^2 X_C}{f}}{R^2 + (fX - \frac{X_C}{f})^2} \quad (8)$$

If the load is capacitive, Equations (6), (7) and (8) will be modified as following:

$$R_L - jX_L = \frac{\left( R - j\frac{X}{f} \right) \left( -j\frac{X_C}{f} \right)}{R - j\frac{X + X_C}{f}} \quad (9)$$

$$R_L = \frac{\frac{R X_C}{f^2} (X + X_C) - \frac{R X X_C}{f^2}}{R^2 + \left( \frac{X + X_C}{f} \right)^2} \quad (10)$$

$$X_L = \frac{\frac{R^2 X_C}{f} + \frac{X X_C}{f^3} (X + X_C)}{R^2 + \left(\frac{X + X_C}{f}\right)^2} \quad (11)$$

Now  $R_1$  and  $R_L$  may be lumped into  $R_{1L} = R_1 + R_L$  and  $fX_{11}$  and  $X_L$  into  $X_{1L} = fX_{11} - X_L$  to obtain the simplified equivalent circuit in Fig. 4.

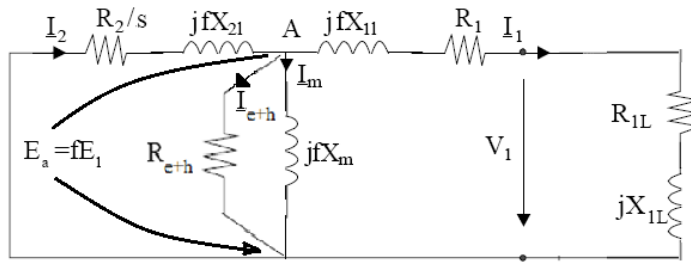


Fig. 4: A simple nodal form of SEIG equivalent circuit

Notice that frequency  $f$  will be given and the new unknowns are  $s$  and  $X_{m-s}$  while  $E_1(I_m)$  or  $X_m(E_1)$  comes from the no-load curve of IG. Also the load resistance and reactance  $R, X$ , the capacitance  $C$  and the values of  $R_2, X_{21}, R_1$  and  $X_{11}$  are given. Consequently, with  $f$  known and  $s$  calculated, the speed  $v$  will be computed as:

$$v = f(1 - s) \quad (12)$$

If the speed is known, a simpler iterative procedure is required to change  $f$  until the desired  $v$  is obtained.

For self-excitation, the summation of currents in node A (Fig. 4) must be zero (implicitly  $E_1 \neq 0$ ).

$$-I_2 + I_m + I_{e+h} + I_1 = 0 \quad (13)$$

$$fE_1 \left( \frac{1}{\frac{R_2}{s} + jfX_{21}} + \frac{1}{jfX_{m-s}} + \frac{1}{R_{e+h}} + \frac{1}{R_{1L} + jX_{1L}} \right) \quad (14)$$

The real and imaginary parts of (10) have to be zero:

$$\frac{sR_2}{R_2^2 + s^2 f^2 X_{21}^2} + \frac{1}{R_{e+h}} + \frac{R_{1L}}{R_{1L}^2 + X_{1L}^2} = 0 \quad (15)$$

$$-\frac{s^2 f X_{21}}{R_2^2 + s^2 f^2 X_{21}^2} - \frac{1}{f X_{m-s}} - \frac{X_{1L}}{R_{1L}^2 + X_{1L}^2} = 0 \quad (16)$$

For a given  $f$ , load and IG parameters, (15) has the slip  $s$  as the only unknown.

$$as^2 + bs + c = 0 \quad (17)$$

$$a = f^2 X_{21}^2 (R_{e+h} R_{1L} + R_{1L}^2 + X_{1L}^2) \quad (18)$$

$$b = R_2 R_{e+h} (R_{1L}^2 + X_{1L}^2) \quad (19)$$

$$c = R_2^2 (R_{e+h} R_{1L}^2 + R_{1L}^2 + X_{1L}^2) \quad (20)$$

Equation (17) has two solutions but only the smaller one ( $s_1$ ) refers to a real generator mode. The larger one refers to a braking regime (all the power is consumed in the machine losses).

$$s_{1,2} = \frac{-b \pm \sqrt{b^2 - 4ac}}{2a} < 0 \quad (21)$$

Complex solutions  $s_{1,2}$  imply that self-excitation cannot take place.

Once  $s_1$  is known, the corresponding speed  $v$ , for a given frequency  $f$ , capacitance and load, is calculated from (12).

When the speed is given,  $f$  is changed until the desired speed  $v$  is obtained.

Now, with  $s, f$ , etc., known, the only unknown in (16) is  $X_{m-s}$ , which is given by:

$$X_{m-s} = \frac{-1}{f \left( \frac{s^2 f X_{21}}{R_2^2 + s^2 f^2 X_{21}^2} + \frac{X_{1L}}{R_{1L}^2 + X_{1L}^2} \right)} \quad (22)$$

If the value of saturated magnetizing reactance  $X_{m-s}$  is either negative or greater than maximum saturated magnetizing reactance  $X_m$ , self-excitation will not take place.

With  $X_{m-s}$  determined,  $E_1$  can be directly obtained from the no-load curve at the rated frequency (Fig. 5).

The relationship between the saturated magnetizing reactance  $X_{m-s}$  and the airgap voltage  $E_1$  in Fig. 5, can be fitted as following:

$$X_{m-s} = M_0 + M_1 E_1 + M_2 E_1^2 \quad (23)$$

where  $M_0, M_1$  and  $M_2$  are constants dependent on the design and material of the machine.

Consequently  $E_1$  can be calculated as the larger solution of quadratic equation in (23).

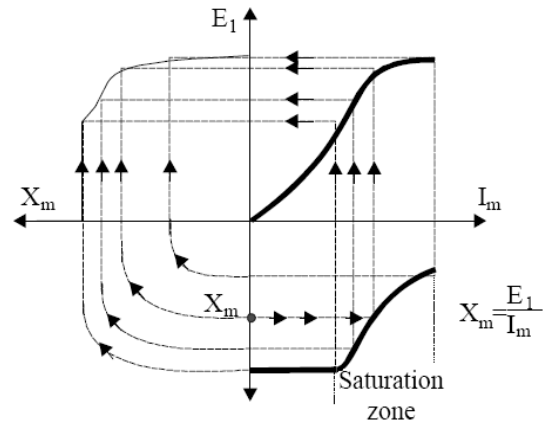


Fig. 5: No-load curve of IG at rated frequency

As  $E_1$  and  $f, s, X_{m-s}$  are known, from the parallel equivalent circuit of Figure 3,  $I_2$  and  $I_1$  can be simply calculated, as  $I_m$  comes directly from the magnetization curve (Fig. 5).

$$I_2 = \frac{-fE_1}{\frac{R_2}{s} + jfX_{21}} \quad (24)$$

$$I_1 = \frac{fE_1}{R_{1L} + jX_{1L}}; \quad X_{1L} < 0 \quad (25)$$

It is now simple to construct the terminal voltage phasor  $V_1$  as in (26).

$$V_1 = fE_1 - I_1(R_1 + jfX_{11}) \quad (26)$$

Capacitor and load currents,  $I_C$  and  $I_L$  are, respectively:

$$I_C = \frac{V_1}{-j \frac{X_C}{f}} \quad (27)$$

$$I_L = I_1 - I_C \quad (28)$$

The output power  $P_{out}$  is given by (29).

$$P_{out} = 3R_L I_L^2 \quad (29)$$

As soon as computerized, the rather straightforward computation procedure presented here allows for all performance computation, for given frequency  $f$  (or speed), capacitance, load and machine parameters. Any load can be handled directly putting it in form of series impedance.

In the case when the speed  $v$ , instead of  $f$ , is fixed, the problem may be solved the same way through a few iterations by changing  $f$  in (17) until the value of  $s < 0$  will produce the required speed  $v = f(1 - s)$ .

The slip and capacitor problem occurs when the voltage  $V_1$ , speed and load are given. To retain simplicity in the computation process, the same algorithm as above may be used repeatedly for a few values of frequency and then for capacitance (above the no-load value at same voltage) until the required voltage and speed are obtained.

The iterative procedure converges rapidly as voltage in general increases with capacitance  $C$ .

## V. PROPOSED ALGORITHM

The computational procedure of iterative method for solution of  $s_1$  and  $X_m$  and subsequent performance of SEIG using MATLAB are as follows:

**Step 1:** Read base impedance and base frequency ( $f_b = f_s$ ).

**Step 2:** Read the machine data ( $R_1, X_1, R_{21}, X_{21}, X_m$ ), load data ( $R, X$ ) and self excitation capacitance ( $C$ ).

**Step 3:** Calculate the resistances, reactances and frequency in per unit.

**Step 4:** Read the initial value of  $E_1$ .

**Step 5:** Calculate  $R_{e+th}$  in per unit using (8).

**Step 6:** Calculate  $a, b$  and  $c$  (the coefficients of (14)) using (15), (16) and (17) respectively.

**Step 7:** Calculate slip  $s_1$  using (18).

**Step 8:** If  $s_1$  is complex value, set  $E_1 = 0$  and go to Step 15.

**Step 9:** Calculate per unit speed using (9).

**Step 10:** Calculate  $X_{m-s}$  using (19).

**Step 11:** If  $0 < X_{m-s} < X_m$  calculate  $E_1$  as the larger solution of quadratic equation in (20). Else set  $E_1 = 0$  and go to Step 15.

**Step 12:** If  $E_1$  is complex value set  $E_1 = 0$  and go to Step 15.

**Step 13:** If the present and previous values of  $E_1$ , are not equal, go to Step 5.

**Step 14:** Calculate  $I_1, V_1$  and  $P_{out}$  using (22), (23) and (26) respectively.

**Step 15:** Stop.

## VI. RESULTS

In this paper, the computed results were obtained by the proposed algorithm outlined above. The experimental results were obtained using a 3-phase induction machine coupled with a separately excited DC motor. The induction machine is a three-phase, star connected stator winding. The induction machine is coupled to a DC motor to provide different constant speeds. Three star connected capacitors of 100  $\mu\text{F}$  per phase, were connected to the machine terminals to obtain self-excited induction generator action.

The induction machine details, the DC machine details and the base values are in Appendix I, II and III respectively.

### A. Terminal Capacitance Requirement of SEIG

The minimum self excitation capacitance  $C_{min}$  (corresponding to  $X_{C-max}$ ) for different speeds at no load, can be obtained using (16). Thus by putting  $R = \infty$  and  $X = 0$  in both of (7) and (8) then  $R_L = 0$  and  $X_L = X_{C-max} / f$ . Hence  $X_{1L} = fX_1 - X_{C-max} / f$  and  $R_{1L} = R_1$ . Because slip has very small value at no load ( $s = 0$ ) then  $v = f(1 - s) = f$ . If  $X_{m-s}$  is replaced with  $X_m$  in (16), the resultant equation will

be quadratic equation and  $X_{C-max}$  is the larger solution as following:

$$X_{C-max} = \frac{v^2}{2} \left[ X_m + 2X_1 + \sqrt{X_m^2 - \frac{4R_1^2}{v^2}} \right] \quad (30)$$

$$C_{min} = \frac{1}{2\pi f_b X_{C-max} Z_b} \quad (31)$$

Fig. (6) shows the calculated results of relationship between  $C_{min}$  and  $v$  using (30) and (31). It is obvious that  $C_{min}$  strongly decreases as the speed rises. This means that a wider speed operating range is achieved using a higher capacitance value.

The value of  $C_{min}$  calculated above, is just sufficient to have self excitation under steady state. If a terminal capacitor  $C = C_{min}$  is used and the generator is started from rest, the voltage build up will not take place. Thus in practice, terminal capacitor  $C$  having a value greater than  $C_{min}$  should be selected to ensure self excitation.

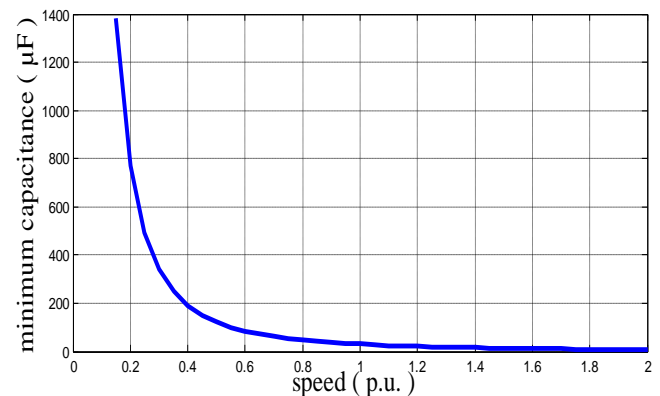


Fig. 6: Minimum self excitation capacitance against speed

Solution of (30) has to be real, so  $v$  has to be greater than critical speed  $v_{critical}$ .

$$v_{critical} = \frac{2R_1}{X_m} \quad (32)$$

There is a speed threshold below which no excitation is possible what the capacitance value. This threshold is called cutoff speed  $v_{cutoff}$ . Cutoff speed  $v_{cutoff}$  is derived in [13] as following:

$$v_{cutoff} = \frac{2R_1}{X_m} \sqrt{\frac{R_1}{R_2} + \left(1 + \frac{X_{21}}{X_m}\right)^2} \quad (33)$$

Anyway cutoff speed is greater than critical speed, so exceeding critical speed is guaranteed.

Cutoff speed for the induction generator under investigation in this paper,  $v_{cutoff} = 0.07$  p.u. (105 rpm).

### B. Generated Frequency of SEIG

The generated frequency versus speed at no load is plotted in Fig. 7. The curves start at speed  $v = 0.55$  p.u. (825 rpm) because under this speed, the induction generator cannot be excited by capacitor of 100  $\mu\text{F}$  per phase. The value of  $v = 0.55$  p.u. can be explored using Fig. 6 through finding the speed value corresponding to  $C_{min} = 100$   $\mu\text{F}$ .

On the other hand, the curves in Figure 7 terminate at speed  $v = 0.8$  p.u. (1200 rpm) because over this speed, the induction generator is heavily overloaded by capacitor of 100  $\mu\text{F}$  per phase.

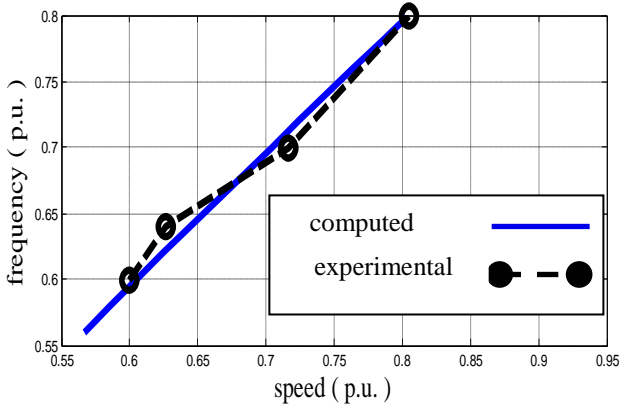


Fig. 7: Generated frequency versus speed at no load

The experimental results are shown on the plots of Fig. 7. It is obvious that there is a good agreement between the experimental and computed results.

The generated frequency versus speed at  $R=150 \Omega$  is plotted in Fig. 8.

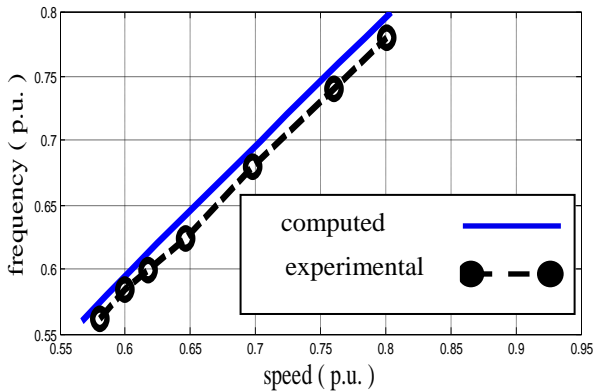


Fig. 8: Generated frequency versus speed at  $R=150 \Omega$

Fig. 9 shows the computed results of relationship between generated frequency and speed at constant capacitor  $C = 150 \mu F$  for resistive, inductive and capacitive loads. As shown, the frequency is affected only a little by the power factor for given load.

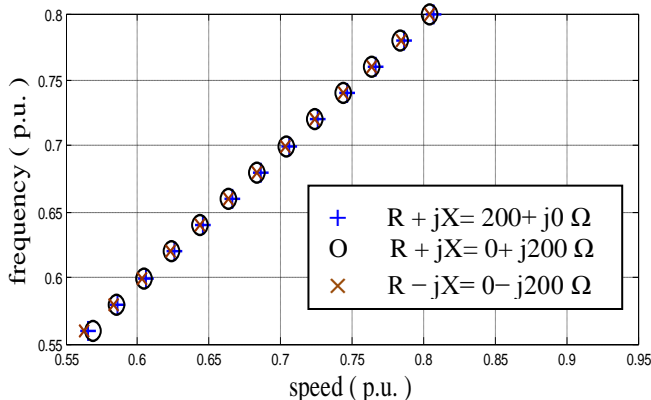


Fig. 9: Generated frequency versus speed at resistive, inductive and capacitive loads

### C. Generated Voltage of SEIG

The generated voltage versus speed at no load is plotted in Fig. 10. The curves starts at speed  $v = 0.55$  p.u. (825 rpm) and terminates at speed  $v = 0.8$  p.u. (1200 rpm) because the same reasons mentioned previously about Fig. 7.

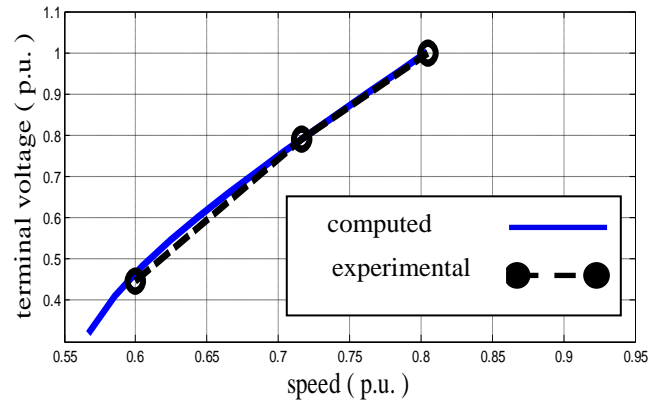


Fig. 10: Generated voltage versus speed at no load

The generated voltage versus speed at  $R=150 \Omega$  is plotted in Fig. 11.

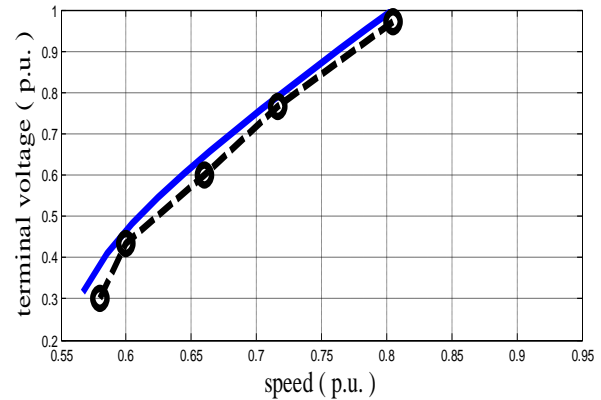


Fig. 11: Generated voltage versus speed at  $R=150 \Omega$

Fig. 12 shows the computed results of relationship between the terminal voltage and speed at constant capacitor  $C = 150 \mu F$  for resistive, inductive and capacitive loads. As shown, the voltage of SEIG is the largest for capacitive load, afterwards resistive load, while on the contrary inductive load is the least. This happens because the load reactance affects the equivalent capacitive reactance.

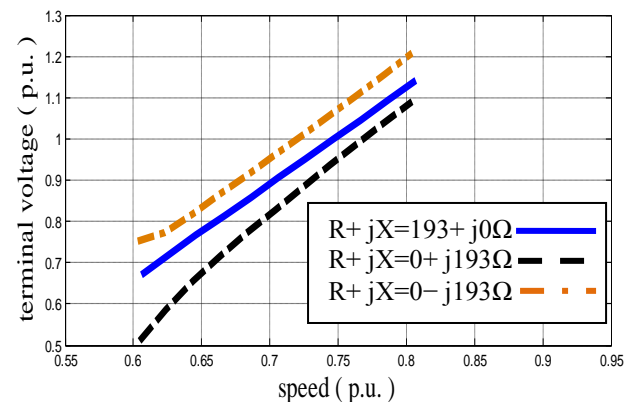


Fig. 12: Generated voltage versus speed at resistive, inductive and capacitive loads

### D. Steady State Characteristics of SEIG

The main steady state characteristics of SEIG are to be obtained at constant capacitor and constant speed. In spite of the fact that a prime mover (such as a small hydroturbine) does not have constant speed if unregulated.

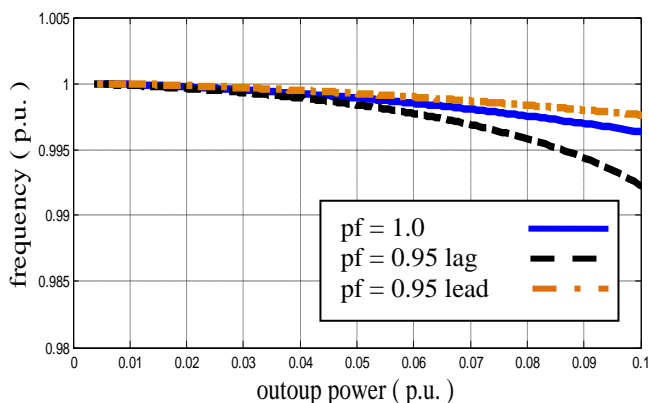


Fig. 13: Generated frequency versus output power for given speed, capacitor and power factor

Fig. 13 shows the computed results of relationship between generated frequency and output power at constant speed  $v = 1.0067$  p.u. (1510 rpm) and constant capacitor  $C = 40 \mu\text{F}$  for unity, leading and lagging load power factor. The frequency scale is excessively reduced to display the differences between curves. As mentioned previously, the frequency is influenced only a little by the power factor for given load.

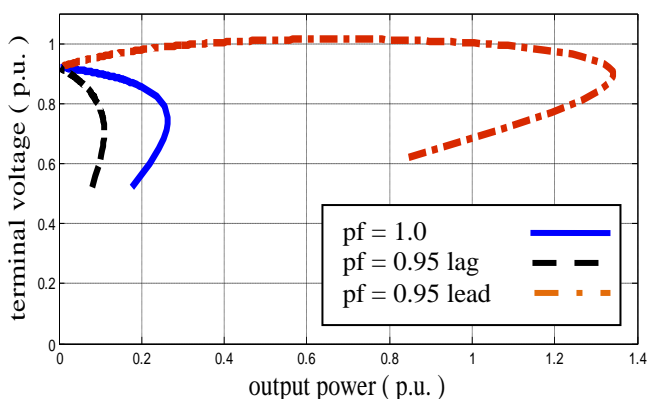


Fig. 14: Generated voltage versus power for given speed, capacitor and power factor

Fig. 14 shows the computed results of relationship between terminal voltage and output power at constant speed  $v = 1$  p.u. (1500 rpm) and constant capacitor  $C = 40 \mu\text{F}$  for unity, leading and lagging load power factor. The slight increase and then decrease in output voltage with output power for leading power factor is expected because the load capacitance increases the equivalent capacitive reactance. For lagging power factor, the voltage drops rapidly because the load inductance decreases the equivalent capacitive reactance and thus the critical slip is achieved at lower power levels.

The characteristics notably change if the prime mover speed is not regulated. The same methodology as above may be used to obtain results.

For constant head hydroturbines, the speed decreases with output power and thus the voltage regulation is even more pronounced. Variable capacitance is needed to limit the voltage regulation.

### CONCLUSIONS

In this paper, the steady state analysis of SEIG is investigated using admittance model. The core loss resistance was taken into account, contrary to most of previous papers.

The proposed analysis gives an opportunity to control the terminal voltage and generated frequency by adjusting speed and capacitor. This supports the implementation of such

generators successfully in wind energy system and micro hydro plant.

The steady-state characteristics show that loading capacity of SEIG is the largest for capacitive load, afterwards resistive load, while on the contrary inductive load is the least.

Closeness between the experimental and computed results, assures the effectiveness and ease of implementation of the proposed method.

### References

- [1] K.S. Sandhu and S. P. Jain, "Steady State Operation of Self-Excited Induction Generator with Varying Wind Speeds", International Journal of Circuits, Systems and Signal Processing, Issue 1, Vol. 2, 2008.
- [2] N. Jenkins, R. Allan, P. Crossley, D. Kirschen, and G. Strbac, "Embedded Generation," The Institute of Electrical Engineers, 2000.
- [3] G. Raina, and O. P. Malik, "Wind Energy Conversion using a Self-Excited Induction Generator," IEEE Transaction on Power Apparatus and Systems, Vol. 102, No. 12, 1983.
- [4] A. K. Sharma, N. P. Patidar, G. Agnihotri and D. K. Palwalia, "Performance Analysis of Self Excited Induction Generator Using Artificial Bee Colony Algorithm," International Journal of Electrical, Computer, Energetic, Electronic and Communication Engineering, Vol. 8, No. 6, 2014.
- [5] Ion Boldea and Syed A. Nasar, "The Induction Machines Design Handbook," Second Edition, CRC Press, Taylor and Francis Group, 2010.
- [6] S. S. Murthy, O. P. Malik and A. K. Tandon, "Analysis of Self-Excited Induction Generators," Proc IEE, Vol. 129C, No. 6, 1982.
- [7] L. Shridhar, B. Singh and C. S. Jha, "A Step Toward Improvements in the Characteristics of Self-Excited Induction Generators," IEEE Trans., Vol. EC-Vol. 8, 1993.
- [8] S. P. Singh, B. Singh and B. P. Jain, "Steady State Analysis of Self-Excited Pole-Changing Induction Generator," The Inst. of Engineering (India), Journal-EL, Vol. 73, 1992.
- [9] S. P. Singh, B. Singh and M. P. Jain, "A New Technique for the Analysis of Self-Excited Induction Generator," EMPS, Vol. 23, No. 6, 1995.
- [10] L. Quazene and G. Mepheron Jr, "Analysis of Isolated Induction Generators," IEEE Trans., Vol. PAS-102, No. 8, 1983.
- [11] N. Ammasaigounden, M. Subbiah, M.R. Krishnamurthy, "Wind Driven Self-Excited Pole-Changing Induction Generators," Proc. IEE, Vol. 133B, No. 5, 1986.
- [12] K. S. Sandhu and S. K. Jain, "Operational Aspects of Self-Excited Induction Generator Using a New Model," EMPS, Vol. 27, No. 2, 1999.
- [13] Shakuntla Boora, "On-Set Theory of Self-Excitation in Induction Generator," International Journal of Recent Trends in Engineering, Vol. 2, No. 5, 2009.

### APPENDIX I

- The details of induction machine are:

#### Specifications

3 phase  
 $2p = 4$  pole  
 $f_s = 50$  Hz  
 $n = 1400$  rpm  
 $V_s = 380$  V

$I_{sn} = 4.5$  A  
 $P_n = 2.4$  hp

#### Parameters

$R_1 = 2.22 \Omega$   
 $R_{21} = 3.1 \Omega$   
 $X_1 = 5 \Omega$   
 $X_{21} = 5 \Omega$   
 $X_m = 99.5 \Omega$

$$M_0 = 2.0269$$

$$M_1 = 0.7508$$

$$M_2 = -1.5373$$

$$N_0 = -4.4178$$

$$N_1 = 19.7584$$

$$N_2 = -3.7166$$

#### APPENDIX II

- The details of DC machine are:

##### Specifications

$$P_n = 2.7 \text{ hp}$$

$$n = 1400 \text{ rpm}$$

$$V_s = 220 \text{ V}$$

$$I_{a_n} = 12 \text{ A}$$

$$V_{f_n} = 220 \text{ V}$$

$$I_{f_n} = 0.8 \text{ A}$$

#### APPENDIX III

- The base values are:

$$V_{b-ph} = 220 \text{ V}$$

$$I_b = 4.5 \text{ A}$$

$$Z_b = 48.89 \Omega$$

$$S_{b-3ph} = 2970 \text{ VA}$$

$$f_b = 50 \text{ Hz}$$

$$n_b = 1500 \text{ rpm}$$